Fin failure diagnosis for non-linear supersonic air vehicle based on inertial sensors

Asghar Ashrafifar[a] and Mohsen Fathi Jegarkandi[*]

Department of Aerospace Engineering, Sharif University of Technology, Tehran, Iran

Abstract. In this paper, a new model-based Fault Detection and Diagnosis (FDD) method for an agile supersonic flight vehicle is presented. A nonlinear model, controlled by a classical closed loop controller and proportional navigation guidance in interception scenario, describes the behavior of the vehicle. The proposed FDD method employs the Inertial Navigation System (INS) data and nonlinear dynamic model of the vehicle to inform fins damage to the controller before leading to an undesired performance or mission failure. Broken, burnt, unactuated or not opened control surfaces cause a drastic change in aerodynamic coefficients and consequently in the dynamic model. Therefore, in addition to the changes in the control forces and moments, system dynamics will change too, leading to the failure detection process being encountered with difficulty. To this purpose, an equivalent aerodynamic model is proposed to express the dynamics of the vehicle, and the health of each fin is monitored by the value of a parameter which is estimated using an adaptive robust filter. The proposed method detects and isolates fins damages in a few seconds with good accuracy.

Keywords: fin failure detection and diagnosis; model aided inertial navigation; parameter estimation; adaptive robust unscented Kalman filter; missile aerodynamics

1. Introduction

Reliability and survivability are very important in tactical aerospace vehicles. The flight control system is one of the subsystems being faced with different faults and malfunctions in sensors, actuators or aerodynamic control surfaces that can lead to performance reduction or failure. To overcome such problems, it is necessary to design control policies which are capable of controlling the system with desired performance even if one or several faults happen in the system. These classes of control systems are known as fault-tolerant control systems (FTCS) (Blanke 1999).

Fault-tolerant control systems can be categorized into two main types: passive fault tolerant controllers (PFTC) and active fault-tolerant controllers (AFTC) (Zhang and Jiang 2008). In PFTC, controllers are fixed and designed to be robust against to a class of presumed faults. In contrast to PFTC, an AFTC includes fault detection and diagnosis (FDD) module and a reconfigurable controller. FDD monitors the health of the system and recognizes unexpected changes in the system former leading to the undesired performance of the system. The FDD informs a supervision module about the occurred fault or damage that decides how to reconfigure the flight controllers.

*Corresponding author, Assistant Professor, E-mail: fathi@sharif.edu
[a]Ph.D. Candidate, E-mail: ashrafimut@gmail.com

The simplest way for fault detection is to use hardware redundancy by employing multiple devices that perform the same role (Johnson 1996). However, in tactical aerospace vehicles, using the redundant hardware is not suitable due to weight and cost constraints. Another strategy is analytical redundancy, which identifies the functional relations between the measured variables via a mathematical model in order to detect malfunctions (Frank 1990). The result is a set of methods called model-based, where the model should be understood as a knowledge-based dynamical model, usually a set of differential equations in the state-space form (Marzat *et al.* 2012).

One of the most widely used methods for FDD is parity space (Gertler and Singer 1990, Patton and Chen 1994, Gertler 1997, Juan 2011, Basri *et al.* 2012). Parity space technique will highlight the consistency between the actual outputs and the normal ones. Besides parity space approach, neural networks, system inversion, state estimation, and parameter estimation are the other methods that have been used by a vast number of researches on fault diagnosis of aerospace vehicle flight control systems (Hanlon and Maybeck 2000, Kun *et al.* 2010, He *et al.* 2017, Meskin *et al.* 2007, Mack *et al.* 2010, Yang *et al.* 2013, Lee *et al.* 2014, Shahrokhi 2015, Lee *et al.* 2016, Lu *et al.* 2017, Crawford *et al.* 2000, Halder *et al.* 2003, Chen 2003, Yu *et al.* 2009, Marzat *et al.* 2010, 2009).

Hanlon and Maybeck (2000) and Kun *et al.* (2010) have developed a Multiple Model Adaptive Estimation (MMAE) algorithm to detect actuator and sensor failures in the flight control system of an aircraft, respectively. The MMAE fault detection and isolation (FDI) consists of parallel Kalman filters and each Kalman filter is constructed to represent a special failure mode. He *et al.* (2017) has proposed a fault-tolerant approach for hypersonic reentry vehicles. In this strategy, when aerodynamic surfaces fail, RCS jets are activated to augment the aerodynamic surfaces to compensate for insufficient torque. An actuator FDI is investigated using a nonlinear longitudinal aircraft model by Meskin *et al.* (2007). In the mentioned paper, two detection filters are designed to estimate the throttle position and the elevator angle, using a collection of estimation models, each corresponding to a system damage situation. Mack *et al.* (2010) have developed a model-based adaptive scheme to detect both system damage and actuator failures in aircraft. Furthermore, the resulting estimation errors can be employed to determine the overall system health situation. A recursive strategy for online detection of actuator faults of an unmanned aerial vehicle was presented by Yang *et al.* (2013). The proposed fault detection strategy consists of a bank of unscented Kalman filters, each of which detects a specific type of actuator faults. Lee *et al.* (2014) have employed a model-matching approach using a bank of adaptive linear unknown input observers based on linearized aircraft models. Shahrokhi (2015) proposed an FDI scheme based on dynamic neural networks and genetic algorithm for thrusters of the autonomous underwater vehicles. A model-based method for FDI of actuator damage and failure on an aircraft was presented by Lee *et al.* (2016). The proposed method is based on multiple linearized models that approximate the nonlinear dynamics of the aircraft and consider uncertainties. Also, Lu *et al.* (2017) proposed an aircraft FTC system, which can maintain controlled flight in the presence of simultaneous sensor and actuator faults.

Besides the aforementioned references, some references tackled the same problem on missiles. A model reference adaptive fin failure tolerant control has been designed by Crawford *et al.* (2000) for the longitudinal missile model. Halder *et al.* (2003) proposed a fault tolerant control scheme using multiple controllers switching in a tactical aerospace vehicle. In this reference, a parity space-based residual generation approach is used to detect fin failure. It employs a limited number of candidate controllers, one of them is to be selected based on the type of faults. A nonlinear disturbance observer-based approach is proposed by Chen (2003) to improve a nonlinear dynamic

inversion control robustness against disturbance and the aerodynamic derivatives uncertainty. Yu *et al.* (2009) proposed a solution based on linear parameter varying fault detection filter for a missile in the cruise phase to detect and isolate the tail actuator and pitch rate sensor fault. An FDI method for a nonlinear control-affine model is presented which employs the redundancy induced by this control module, along with the accelerations by Marzat *et al.* (2010). Also, a model-free fault diagnosis method based on the study of closed-loop control signals has been proposed by Marzat *et al.* (2009).

Patton (1997) and Jiang and Zhao (1997) demonstrate that the state estimation-based algorithms are intrinsically fast and have a short time delay in the real-time decision process, but results are not detailed in comparison with parameter estimation approach. Therefore, a combination of both algorithms is more appropriate.

In the current paper, the problem of missile fin failure detection, including burning, breaking, unactuated, or not opening has been studied. The loss of the missile fins results in a drastic change in the dynamic model that will hamper the detection process. In other words, in addition to the changes in the control forces and moments, system dynamics will change, too. Therefore, to identify model changes after fin failure, the aerodynamics of body and control surfaces are modeled separately. New aerodynamic model will prevent the estimation of all coefficients. A percentage of the fins which have the ability to generate aerodynamic forces are modeled by parameters and these parameters are estimated over time, using a robust estimator to ensure robustness against aerodynamic coefficient uncertainty. The value of these parameters will be between 0 and 1. Where value 1 corresponds to the health of the fin and zero value denotes whether the fin has not opened or has been destroyed completely.

The paper is organized as follows: First, the considered vehicle is introduced and its nonlinear model is derived. The proposed method for identification is discussed, as well. For this purpose, the model is expressed in such a way to detect control fins damages that consist of partial melting or breakage. Next, a brief introduction to unscented Kalman filter (UKF) and Adaptive Robust UKF (ARUKF) is provided. Then, the performance of the new FDD approach is evaluated through numerical simulations. Finally, a summary and conclusion are presented.

2. System description

The system considered in this paper is a Skid-To-Turn (STT) aerodynamic control surface-to-air missile on an interception mission. While the four aerodynamic tail fins act as lifting surfaces and are the control surfaces steering the vehicle. The geometry of the missile in its body frame is illustrated in Fig. 1.

Consider equations of motion for a rigid missile flying in three-dimensional inertial space consisting of translational and rotational motions in body coordinate frame as follows (see Stevens *et al.* 2015):

$$\dot{u} = rv - qw + \frac{1}{m}\left(F_{Tx} + F_{gx} + F_{Ax}\right)$$
$$\dot{v} = pw - ru + \frac{1}{m}\left(F_{Ty} + F_{gy} + F_{Ay}\right) \quad (1)$$
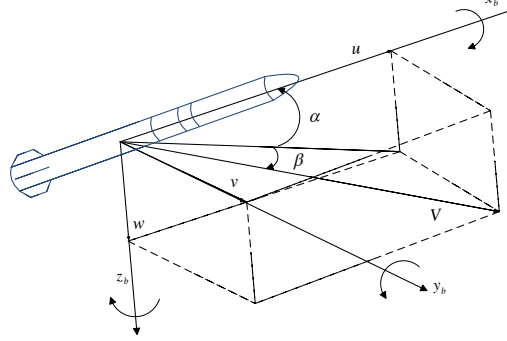$$\dot{w} = qu - pv + \frac{1}{m}\left(F_{Tz} + F_{gz} + F_{Az}\right)$$

and

Fig. 1 Missile body coordinate frame

$$
\begin{aligned}
\dot{p} &= \tfrac{1}{I_x}\left\{(I_y - I_z)\,qr + l_A\right\} \\
\dot{q} &= \tfrac{1}{I_y}\left\{(I_z - I_x)\,rp + m_A\right\} \\
\dot{r} &= \tfrac{1}{I_z}\left\{(I_x - I_y)\,pq + n_A\right\}
\end{aligned}
\tag{2}
$$

where the scalar quantity m represents mass and I_x, I_y and I_z are moments of inertia of the missile about x, y and z axis, respectively. The missile has an axisymmetric, cruciform shape so that the moments of inertia I_y and I_z are identical. Also, u, v, and w, are components of the velocity vector, and p, q and r, represent components of the angular velocity vector, respectively. F_A, F_g, and F_T are vectors for aerodynamic, gravity and thrust forces acting on the vehicle, respectively. Aerodynamic moments are denoted by l_A, m_A, and n_A respectively.

Components of gravity force in body frame are derived using the following equations (Zipfel 2007):

$$
\begin{aligned}
F_{gx} &= -mg\sin(\theta) \\
F_{gy} &= mg\cos(\theta)\sin(\varphi) \\
F_{gz} &= mg\cos(\theta)\cos(\varphi)
\end{aligned}
\tag{3}
$$

where φ, θ and ψ are Euler angles and can be written as (Zipfel 2007):

$$
\begin{aligned}
\dot{\varphi} &= p + q\sin(\varphi)\tan(\theta) + r\cos(\varphi)\tan(\theta) \\
\dot{\theta} &= q\cos(\varphi) - r\sin(\varphi) \\
\dot{\psi} &= q\sin(\varphi)\sec(\theta) + r\cos(\varphi)\sec(\theta)
\end{aligned}
\tag{4}
$$

Eq. (1) is written as the time derivatives of the body axis components of velocity. However, the variables of interest in flight control are the angle of attack and side-slip angle. According to Fig. 1 and some mathematical manipulations, we have:

$$
\begin{aligned}
\dot{\alpha} = q &- [p\cos(\alpha) + r\sin(\alpha)]\tan\beta - \tfrac{\sin(\alpha)}{mV\cos(\beta)}(F_{Ax} + F_{Tx}) + \tfrac{\cos(\alpha)}{mV\cos(\beta)}F_{Az} \\
&+ \tfrac{g}{V\cos(\beta)}[\cos(\theta)\cos(\varphi)\cos(\alpha) + \sin(\theta)\sin(\alpha)]
\end{aligned}
\tag{5}
$$

$$
\begin{aligned}
\dot{\beta} = p\sin(\alpha) &- r\cos(\alpha) - \tfrac{\cos(\alpha)\sin(\beta)}{mV}(F_{Ax} + F_{Tx}) + \tfrac{\cos(\beta)}{mV}F_{Ay} - \tfrac{\sin(\alpha)\sin(\beta)}{mV}F_{Az} \\
&+ \tfrac{g}{V}[\cos(\theta)\sin(\varphi)\cos(\beta) + \sin(\theta)\cos(\alpha)\sin(\beta) - \cos(\theta)\cos(\varphi)\sin(\alpha)\sin(\beta)]
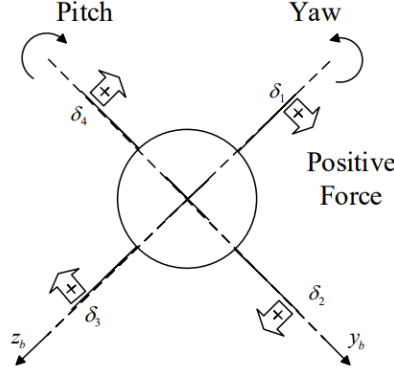\end{aligned}
\tag{6}
$$

Fig. 2 Fin Deflection Sign Convention

$$\dot{V} = \frac{\cos(\alpha)\cos(\beta)}{m}\left(F_{Ax} + F_{Tx}\right) + \frac{\sin(\beta)}{m}F_{Ay} + \frac{\sin(\alpha)\cos(\beta)}{m}F_{Az}$$
$$+g\left[\sin(\beta)\sin(\varphi)\cos(\theta) - \cos(\alpha)\cos(\beta)\sin(\theta) + \sin(\alpha)\cos(\beta)\cos(\varphi)\cos(\theta)\right] \tag{7}$$

Also, aerodynamic forces and moments formulated as follows (Zipfel 2007):

$$\begin{aligned}
F_{Ax} &= C_x\bar{q}s = (C_{xs})\,\bar{q}s \\
F_{Ay} &= C_y\bar{q}s = (C_{ys} + C_{yp}p + C_{yr}r + C_{y\delta_r}\delta_r)\,\bar{q}s \\
F_{Az} &= C_z\bar{q}s = (C_{zs} + C_{zq}q + C_{z\delta_e}\delta_e)\,\bar{q}s \\
l_A &= C_l\bar{q}s = (C_{ls} + C_{lp}p + C_{lr}r + C_{l\delta_a}\delta_a)\,\bar{q}sd \\
m_A &= C_m\bar{q}s = \{C_{ms} + (C_{m\dot{\alpha}} + C_{mq})q + C_{m\delta_e}\delta_e\}\,\bar{q}sd \\
n_A &= C_n\bar{q}s = (C_{ns} + C_{np}p + C_{nr}r + C_{n\delta_r}\delta_r)\,\bar{q}sd
\end{aligned} \tag{8}$$

where $\bar{q}$, s and d are dynamic pressure, reference area and reference length, respectively. C_x, C_y, C_z, C_l, C_m and C_n are static force and moment aerodynamic coefficients. C_{lr}, C_{nr} and C_{yr} are rolling moment, yawing moment and side force coefficient derivatives with respect to yaw rate. C_{lp}, C_{np} and C_{yp} are rolling moment, yawing moment and side force coefficient derivatives with respect to roll rate. C_{mq} and C_{zq} are pitching moment and normal force coefficient derivatives with respect to pitch rate. $C_{m\dot{\alpha}}$ is pitching moment coefficient derivative with respect to rate of change of angle of attack. Also, $C_{z\delta e}$, $C_{y\delta r}$, $C_{l\delta a}$, $C_{m\delta e}$ and $C_{n\delta r}$ are control force and moment coefficients derivatives with respect to δ_a, δ_e and δ_r which are aileron, elevator and rudder deflections respectively.

The sign convention corresponding to the fin deflection angles has been shown in Fig. 2, and is as a positive panel normal force producing a positive roll moment (Hemsch 1992).

Therefore, according to the sign convention, positive roll, pitch, and yaw moments will be created using the following mixing logic:

$$\begin{aligned}
\delta_a &= \tfrac{1}{4}\left(+\delta_1 + \delta_2 + \delta_3 + \delta_4\right) \\
\delta_e &= \tfrac{1}{2}\left(+\delta_2 - \delta_4\right) \\
\delta_r &= \tfrac{1}{2}\left(-\delta_1 + \delta_3\right)
\end{aligned} \tag{9}$$

In the next section, the dynamic model will be expressed in a manner which is suitable for the failure detection module.

3. Failure detection and diagnosis scheme

Damaged or not opening aerodynamic control fins caused two types of changes in the aerodynamic model. A change occurs in the number of aerodynamic control coefficients that create new coupling coefficients; for example, if fin number 1 is damaged, elevator deflection would cause a roll, too. Another effect is caused by a change in configuration and vehicle asymmetry, in which the static and dynamic aerodynamic coefficients change as well.

So, for fin failure detection and diagnosis another formulation is introduced that is appropriate for this purpose. In this model, the aerodynamics of the airframe and fins are modeled separately. This procedure isolates possible changes from the damage of fins and show their effects in the simulation. In contrast, if the conventional aerodynamic model has been used, then all coefficients must be estimated to detect the failure and to repair the controller. To avoid this, the aerodynamics of the airframe and fins are modeled separately as follows:

$$
\begin{bmatrix} C_x \\ C_y \\ C_z \end{bmatrix} = \begin{bmatrix} C_{x\,body} \\ C_{y\,body} \\ C_{z\,body} \end{bmatrix} + \sum_{i=1}^{4} \lambda_i \begin{bmatrix} C_{x\,fin\,i} \\ C_{y\,fin\,i} \\ C_{z\,fin\,i} \end{bmatrix} \tag{10}
$$

$$
\begin{bmatrix} C_l \\ C_m \\ C_n \end{bmatrix} = \begin{bmatrix} C_{l\,body} \\ C_{m\,body} \\ C_{n\,body} \end{bmatrix} + \sum_{i=1}^{4} \lambda_i \left(\begin{bmatrix} r_{xi} \\ r_{yi} \\ r_{zi} \end{bmatrix} \times \begin{bmatrix} C_{x\,fin\,i} \\ C_{y\,fin\,i} \\ C_{z\,fin\,i} \end{bmatrix} \right) \tag{11}
$$

where $[r_{xi}, r_{yi}, r_{zi}]^{\mathrm{T}}$ is the distance vector from the vehicle mass center to the ith fin aerodynamic center. The parameters λ_i determine the efficiency of the fins and the value of them will be between 0 and 1. Where value 1 means the health of the fin and zero value indicates whether the fin has not opened or has been damaged completely.

Aerodynamic coefficients are generated by missile DATCOM (Rosema *et al.* 2011). Two DATCOM models are created to determine the effects of the body and fins. The first model includes only the body and ogive nose. Fins are added to the second model. Results are compared to the first model and the difference in the aerodynamic coefficients represents the contribution of fins. In Table 1, aerodynamic coefficients for a given flight condition are compared, for both considered models. As can be seen, the difference is overally negligible and in the worst case is below 10%.
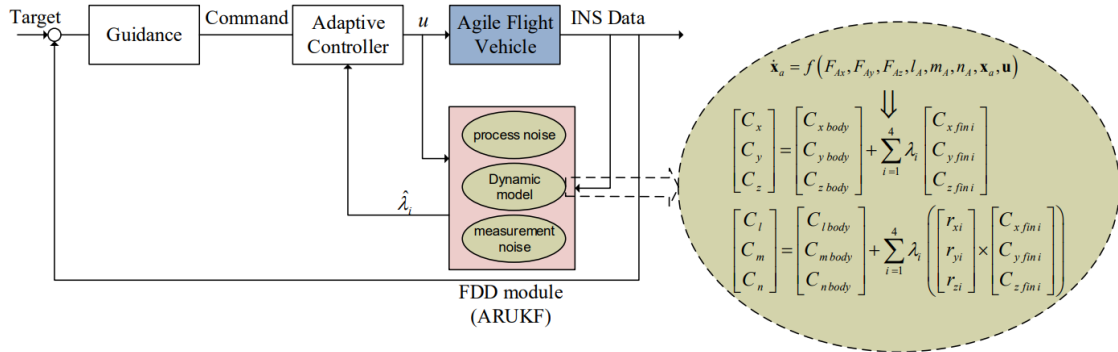

Fig. 3 Failure tolerant control block diagram

The goal is to identify λ_i over time using filter estimator. In this paper, an adaptive robust unscented Kalman filter has been used. The proposed diagnosis module is shown in Fig. 3.

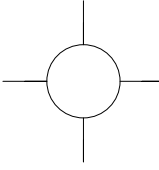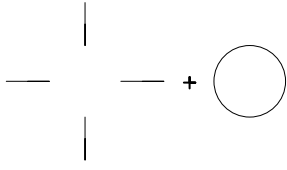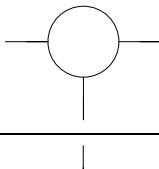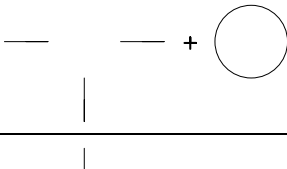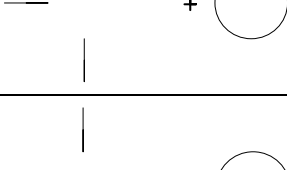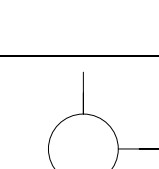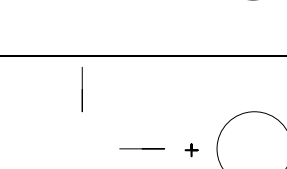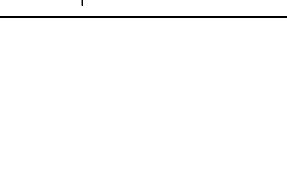## 4. Parameter estimation using adaptive robust unscented Kalman filter structures

The system dynamics is represented in state space form as follows:

$$\dot{\mathbf{x}} = f(\mathbf{x}, \lambda, t) + g(\mathbf{x}, \lambda, t)\mathbf{u}$$
$$\mathbf{y} = h(\mathbf{x}, t) \tag{12}$$

where $\mathbf{x} = [\alpha, \beta, V, p, q, r, \varphi, \theta]^T$ is the state vector with initial value x_0 at time t_0, $\mathbf{u} = [\delta_1, \delta_2, \delta_3, \delta_4]^T$ is the input vector, $\mathbf{y}$ is the INS data including acceleration and angular velocity of the missile.

Parameters estimation through the filtering approach is an indirect procedure, consisting of transforming the problem into a state estimation problem. This is done by augmenting the system

Table 1 Comparison of aerodynamic coefficients calculated by two considered model in a flight condition ($\alpha = 10$ deg, $\beta = 5$ deg, $V_M = 1200$ m/s, $[p, q, r] = [0.5\ 1.5\ 1.0]$ rad/s, $[\delta_a, \delta_e, \delta_r] = [10\ 20\ -30]$ deg)

Conventional model	coefficients	proposal model for failure detection	coefficients	Difference (%)
	$C_x = -0.315$		$C_x = -0.315$	0.0
	$C_y = -4.38$		$C_y = -4.378$	0.05
	$C_z = -4.929$		$C_z = -4.928$	0.02
	$C_l = -1.81$	+	$C_l = -1.96$	8.3
	$C_m = -18.2$		$C_m = -17.91$	1.6
	$C_n = 20.7$		$C_n = 20.44$	1.25
	$C_x = -0.2988$		$C_x = -0.2987$	0.03
	$C_y = -2.052$		$C_y = -2.016$	1.7
	$C_z = -4.929$		$C_z = -4.928$	0.02
	$C_l = 0.255$	+	$C_l = 0.2731$	7.1
	$C_m = -18.2$		$C_m = -17.91$	1.6
	$C_n = 6.57$		$C_n = 6.30$	4.1
	$C_x = -0.2988$		$C_x = -0.2987$	0.03
	$C_y = -4.380$		$C_y = -4.378$	0.05
	$C_z = -2.632$		$C_z = -2.657$	0.95
	$C_l = 0.2133$	+	$C_l = 0.2152$	0.9
	$C_m = -4.235$		$C_m = -4.279$	1.03
	$C_n = 20.7$		$C_n = 20.44$	1.25
	$C_x = -0.2988$		$C_x = -0.2987$	0.03
	$C_y = -3.008$		$C_y = -3.044$	1.2
	$C_z = -4.929$		$C_z = -4.928$	0.02
	$C_l = -3.024$	+	$C_l = -3.29$	8.7
	$C_m = -18.2$		$C_m = -17.91$	1.5
	$C_n = 12.38$		$C_n = 12.43$	0.4
	$C_x = -0.2988$		$C_x = -0.2987$	0.03
	$C_y = -4.380$		$C_y = -4.378$	0.05
	$C_z = -3.71$		$C_z = -3.685$	0.7
	$C_l = -2.873$	+	$C_l = -3.121$	8.6
	$C_m = -10.78$		$C_m = -10.45$	3.06
	$C_n = 20.7$		$C_n = 20.44$	1.25

state vector by defining the unknown parameters (λ_i) as additional state variables.

Now, we consider the constant parameters λ_i as augmented state vector presented below,

$$\dot{\lambda}_\mathbf{i} = 0, \tag{13}$$

Then, the augmented state vector is defined as:

$$\mathbf{x}_a = \begin{bmatrix} \mathbf{x} \\ \lambda_i \end{bmatrix} \tag{14}$$

UKF is a recursive minimum mean square error (MMSE) estimator, first proposed by Julier and Uhlmann (1997). UKF uses a deterministic sampling technique, known as unscented transform to generate a minimal set of sample points around the mean. These points completely capture the mean and covariance of the Gaussian random variable, and when propagated using the nonlinear system equations, capture the posterior mean and covariance accurately to the 3rd order for any nonlinearity (Van Der Merwe *et al.* 2001). The result is a filter which more accurately captures the mean and covariance for nonlinear systems. This technique removes the requirement to explicitly calculate Jacobians, which is difficult for complex functions.

One of the uncertainties that exist in the model of a flight vehicle flying inside the atmosphere is the uncertainty of the aerodynamic coefficients. Ishihara and Yamakita (2016) proposed an adaptive robust UKF (ARUKF) for the state estimation of a nonlinear system with parameter uncertainties. Therefore, we used ARUKF to ensure robustness against the variation of aerodynamic derivatives of the model dynamic. In the following, the ARUKF algorithm is described briefly (see Ishihara and Yamakita 2016). If α_k is set to zero, in Eq. (22), the conventional UKF results. Consider a nonlinear system with parameter uncertainties:

$$\begin{aligned} \mathbf{x}_k &= f(\mathbf{x}_{k-1}, \mathbf{p}_{k-1}) + \mathbf{w}_k \\ \mathbf{y}_k &= \mathbf{H}_k \mathbf{x}_k + \mathbf{v}_k \end{aligned} \tag{15}$$

where the vector $\boldsymbol{x}_k \in \mathbb{R}^n$, $\boldsymbol{y}_k \in \mathbb{R}^m$ and $\boldsymbol{p}_k \in \mathbb{R}^\ell$ represent states, measurements and parameter uncertainties. Also, $\boldsymbol{w}_k$ and $\boldsymbol{v}_k$ are uncorrelated zero-mean Gaussian white process noise and measurement noise and their covariances are $\mathbf{Q}_k$ and $\mathbf{R}_k$ respectively. We assume the distribution of parameter uncertainties is known as $\boldsymbol{p}_k \sim \mathcal{N}(\boldsymbol{p}_k^{nom}, \boldsymbol{p}_k^{pp})$.

- Predictive step:

First, define weights as:

$$\begin{aligned} \mathcal{W}_0^{(m)} &= \frac{\lambda_{ukf}}{n + \lambda_{ukf}} \\ \mathcal{W}_0^{(c)} &= \mathcal{W}_0^{(m)} + (1 - \alpha_{ukf}^2 + \beta_{ukf}) \\ \mathcal{W}_i^{(c)} &= \mathcal{W}_i^{(m)} = \frac{1}{2(n + \lambda_{ukf})}, \quad for \ \ i = 1, ..., n \end{aligned} \tag{16}$$

The complete discussion on how to choose the weighting parameters is presented by Crassidis and Junkins (2004). For Gaussian, $\beta_{ukf} = 2$ and $(n + \lambda_{ukf}) = 3$ are optimal choice.

Now, generate $2n + 1$ sigma point:

$$\chi_{k-1|k-1} = \begin{bmatrix} \hat{\mathbf{x}}_{k-1|k-1} \\ \hat{\mathbf{x}}_{k-1|k-1} + \sqrt{(n + \lambda_{ukf})\hat{\mathbf{P}}_{k-1|k-1}^{xx}} \\ \hat{\mathbf{x}}_{k-1|k-1} - \sqrt{(n + \lambda_{ukf})\hat{\mathbf{P}}_{k-1|k-1}^{xx}} \end{bmatrix} \tag{17}$$

Predictive mean and covariance are shown as following:

$$\hat{\mathbf{x}}_{k|k-1} = \sum_{i=0}^{2n} \mathcal{W}_i^{(m)} \chi_{k|k-1,i} \tag{18}$$

$$\mathbf{P}_{k|k-1}^{xx} = \sum_{i=0}^{2n} \mathcal{W}_i^{(c)} \left(\chi_{k|k-1,i} - \hat{\mathbf{x}}_{k|k-1}\right) \left(\chi_{k|k-1,i} - \hat{\mathbf{x}}_{k|k-1}\right)^{\mathrm{T}} + \mathbf{Q}_k \tag{19}$$

where $\chi_{k|k-1,i} = f\left(\chi_{k-1|k-1,i}\right)$.

Calculated influence of parameter uncertainties

$$\mathbf{F}_{p,k-1} = \left\{ \sum_{j=0}^{2\ell} \mathcal{W}_j f\left(\hat{\mathbf{x}}_{k|k-1}, \mathrm{P}_j\right) \left(\mathrm{P}_j - p_{k-1}^{norm}\right)^{\mathrm{T}} \right\} \{\mathbf{P}_k^{pp}\}^{-1} \tag{20}$$

where $\boldsymbol{P}_j$ are sigma points sampled from $\mathcal{N}(\boldsymbol{p}_{k-1}^{nom}, \boldsymbol{p}_{k-1}^{pp})$.

Then, $\hat{\boldsymbol{P}}_{k|k-1}^{rob}$ is defined as

$$\hat{\mathbf{P}}_{k|k-1}^{rob} = \mathbf{F}_{p,k-1} \mathbf{P}_{k-1}^{pp} \mathbf{F}_{p,k-1}^T + \Delta \mathbf{P}_k^{rukf} \tag{21}$$

where $\Delta \boldsymbol{P}_k^{rukf}$ is tuning parameter to ensure the stability of the ARUKF.

Now, using an adaptive parameter α_k ($\alpha_k > 0$), we define a prediction error covariance matrix as

$$\hat{\mathbf{P}}_{k|k-1}^{xx,arukf} = \hat{\mathbf{P}}_{k|k-1}^{xx} + \alpha_k \hat{\mathbf{P}}_{k|k-1}^{rob} \tag{22}$$

where the details of the mathematical derivation of alpha can be found in (Ishihara and Yamakita 2016).

Compute measurement mean and covariance as follows:

$$\hat{\mathbf{y}}_{k|k-1} = \sum_{i=0} \mathcal{W}_i^{(m)} Y_{k|k-1,i} \tag{23}$$

$$\mathbf{P}_{k|k-1}^{yy} = \sum_{i=0}^{2n} \mathcal{W}_i^{(c)} \left(Y_{k|k-1,i} - \hat{\mathbf{y}}_{k|k-1}\right) \left(Y_{k|k-1,i} - \hat{\mathbf{y}}_{k|k-1}\right)^{\mathrm{T}} + \mathbf{R}_k \tag{24}$$

$$\mathbf{P}_{k|k-1}^{xy} = \sum_{i=0}^{2n} \mathcal{W}_i^{(c)} \left(\chi_{k|k-1,i} - \hat{\mathbf{x}}_{k|k-1}\right) \left(Y_{k|k-1,i} - \hat{\mathbf{y}}_{k|k-1}\right)^{\mathrm{T}} \tag{25}$$

where $Y_{k|k-1,i} = h(\chi_{k-1|k-1,i})$.

- Update step:

$$\mathbf{K}_k = \hat{\mathbf{P}}_{k|k-1}^{xy} \left(\hat{\mathbf{P}}_{k|k-1}^{yy}\right)^{-1} \tag{26}$$

$$\hat{\mathbf{x}}_{k|k} = \hat{\mathbf{x}}_{k|k-1} + \mathbf{K}_k \left(\tilde{\mathbf{y}}_k - \hat{\mathbf{y}}_{k|k-1}\right) \tag{27}$$

$$\hat{\mathbf{P}}_{k|k}^{xx} = \hat{\mathbf{P}}_{k|k-1}^{xx} - \mathbf{K}_k \hat{\mathbf{P}}_{k|k-1}^{yy} \mathbf{K}_k^{\mathrm{T}} \tag{28}$$

In order to ensure the filter convergence, the observability of the nonlinear system is analyzed. Identifiably of the parameters can be investigated by observability rank tests viewing parameters as state variables. To this end, if rank of matrix ($\mathbf{O}_{obs}$) equals the number of parameters, then the model of the system described in equation (15) is identifiable (Anguelova 2004).

$$\mathbf{O}_{obs} = \begin{bmatrix} \frac{\partial L_f h_1}{\partial \lambda_1} & \cdots & \frac{\partial L_f h_1}{\partial \lambda_k} \\ \cdots & & \cdots \\ \frac{\partial L_f h_m}{\partial \lambda_1} & \cdots & \frac{\partial L_f h_m}{\partial \lambda_k} \\ \cdots & & \cdots \\ \frac{\partial L_f^{n-1} h_1}{\partial \lambda_1} & \cdots & \frac{\partial L_f^{n-1} h_1}{\partial \lambda_k} \\ \cdots & & \cdots \\ \frac{\partial L_f^{n-1} h_m}{\partial \lambda_1} & \cdots & \frac{\partial L_f^{n-1} h_m}{\partial \lambda_k} \end{bmatrix} \tag{29}$$

where $L_f h$ is the Lie derivative of a function h with respect to a vector field f.

The rank of matrix $\mathbf{O}_{obs}$ for the intended augmented model is 4. This means that all λ_i are observable.

5. Numerical results and analysis

To evaluate the performance of the proposed failure detection strategy, this method is investigated during an interception mission. The surface-to-air missile tries to hit an accelerated target which follows a given path. Interceptor and target initial conditions are summarized in Table 2. After the time T_{Guide} the controller will be active.

To model the errors of accelerometers and gyros, scale factor error (S), bias (B), misalignment (M) and white noise have been considered. For a given IMU, the errors of accelerometers and gyros are assumed as

$$\begin{bmatrix} S_{axx} & M_{axy} & M_{axz} \\ M_{ayx} & S_{ayy} & M_{ayz} \\ M_{azx} & M_{azy} & S_{azz} \end{bmatrix} = \begin{bmatrix} 1.0050 & 0.0002 & 0.0001 \\ 0.0002 & 1.0050 & 0.0002 \\ 0.0001 & 0.0002 & 1.0050 \end{bmatrix}$$

$$\begin{bmatrix} B_{ax} \\ B_{ay} \\ B_{az} \end{bmatrix} = \begin{bmatrix} 0.0005 \\ 0.0005 \\ 0.0005 \end{bmatrix} m/s$$

$$\begin{bmatrix} S_{gxx} & M_{gxy} & M_{gxz} \\ M_{gyx} & S_{gyy} & M_{gyz} \\ M_{gzx} & M_{gzy} & S_{gzz} \end{bmatrix} = \begin{bmatrix} 0.99995 & 0.00010 & 0.00005 \\ 0.00010 & 1.00050 & 0.00005 \\ 0.00005 & 0.00005 & 0.99995 \end{bmatrix}$$

$$\begin{bmatrix} B_{gx} \\ B_{gy} \\ B_{gz} \end{bmatrix} = \begin{bmatrix} 2 \times 10^{-8} \\ 2 \times 10^{-8} \\ 2 \times 10^{-8} \end{bmatrix} rad/s$$

The variances of accelerometers and gyros white noises are 10^{-6} (m^2/s^4) and 10^{-8} (rad^2/s^2), respectively. Also, it is assumed that the aerodynamic coefficients are available with an accuracy of 10 percent. So, aerodynamic coefficients are parameters with uncertainty for ARUKF.

To demonstrate the effectiveness of the proposed algorithm, three scenarios are investigated. In the first scenario, no failures occur. In scenario 2 it is assumed that 80, 30 and 20 percent of fins No.1, 3

Table 2 The initial conditions

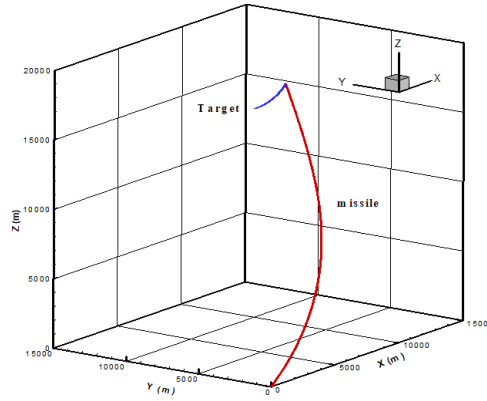|	Position (m)	Speed (m/s)	T_{Guide} (s)
Interceptor	[0; 0; 0]	210	2
Target	[10000; 10000; 15000]	110	-

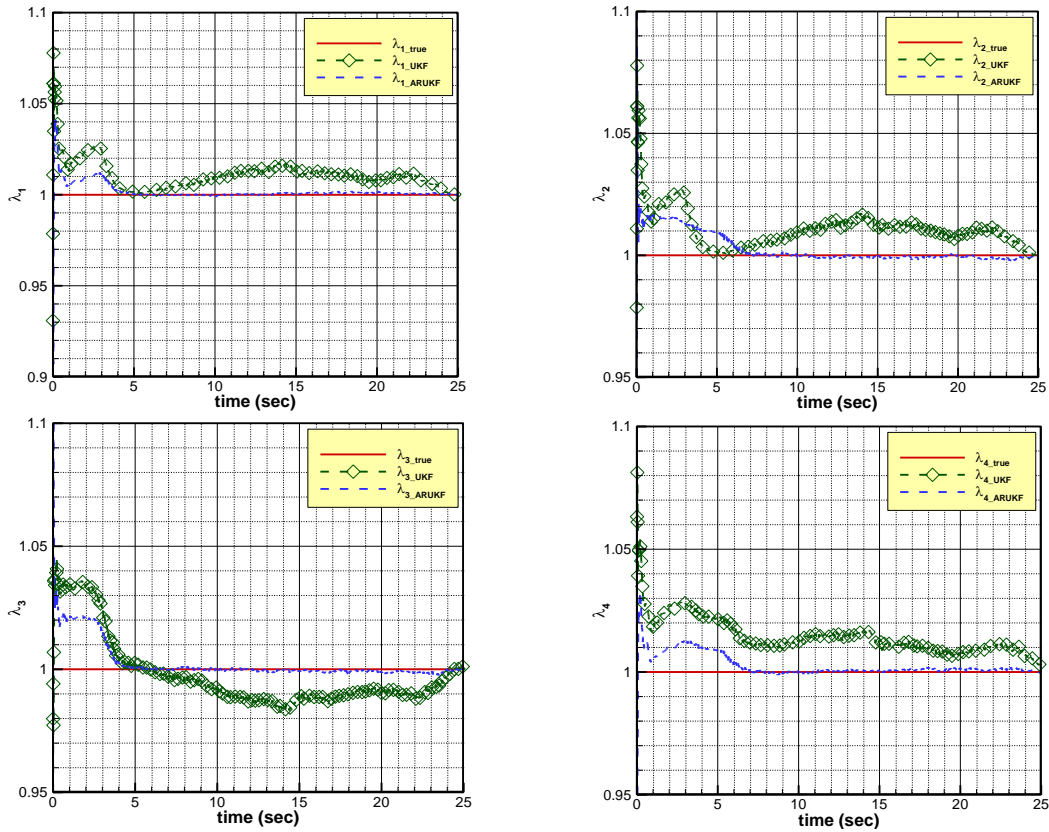Fig. 4 Missile target engagement geometry (scenario 1)

Fig. 5 Percentage of fins which have the ability to generate aerodynamic force for 1000 Monte-Carlo simulation (scenario 1)
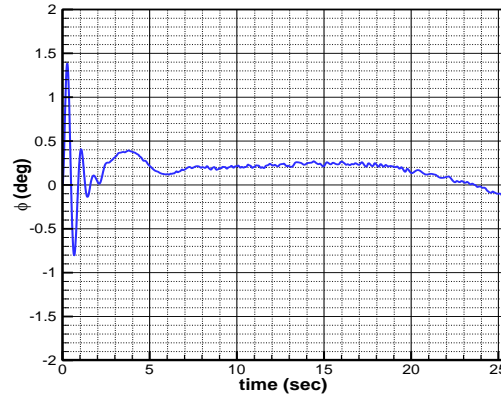
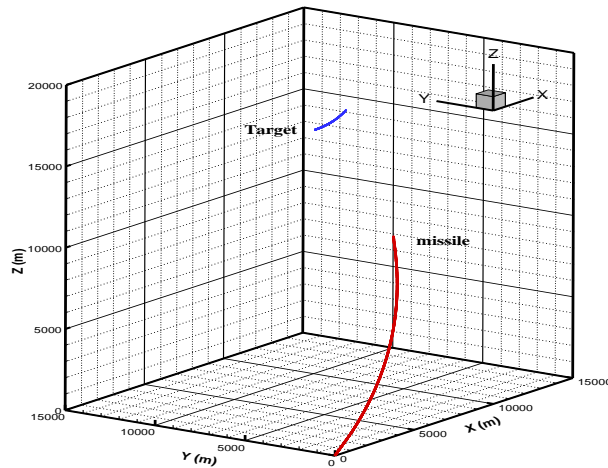Fig. 6 Missile roll angle (scenario 1)

Fig. 7 Missile target engagement geometry (scenario 2)

and 4 have been broken, respectively; and fin No.2 began to melt due to aerodynamic heating. Finally, in the last scenario it is assumed that fin 4 will be destroyed completely 10 seconds after launch. The results are shown in Fig. 4 through Fig. 12, and the norm of estimated error is summarized in the Table 3. The results are for 1000 Monte-Carlo simulation in which the aerodynamic uncertainties are random parameters.

It is shown that in the first scenario, all fins are safe and therefore interceptor hits the target and roll remains about zero. Also, estimator estimates λ_i correctly. Because of the type of seeker, the missile should not roll, and after the fin failure, until the missile has a severe roll, less than 10 degrees, there is time to recognize the failure and inform the controller.

In scenario 2, the percentage of undamaged part of each fin has been estimated with good accuracy. Also, after the failure, the missile rolls about 10 degrees, and after about 5 seconds it becomes unstable and total failure happens. Therefore, instantly after failure occurrence, the λ_i values should be submitted to the controller to determine the appropriate control action. Then, the new control signal should be applied to the system.
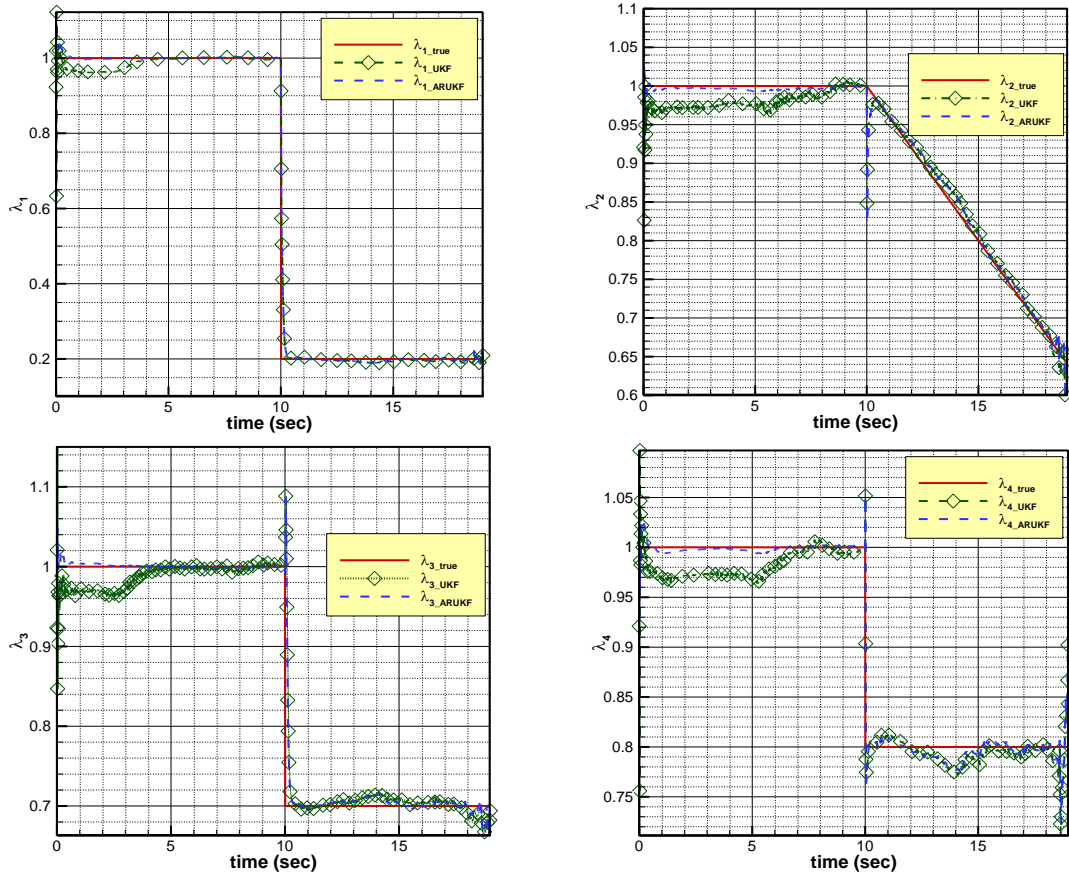
Fig. 8 Percentage of fins which have the ability to generate aerodynamic force for 1000 Monte-Carlo simulation (scenario 2)
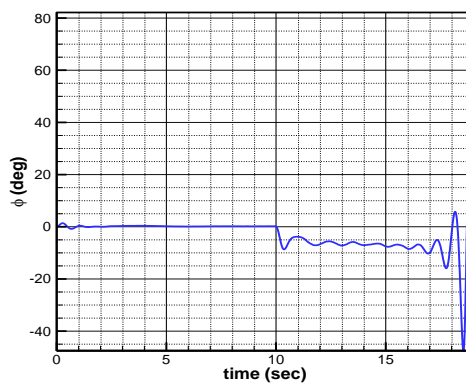

Fig. 9 Missile roll angle (scenario 2)

Finally, in the last scenario, the complete destruction of one fin is investigated. As can be seen, the filter estimates zero value for λ_4 properly and quickly. It should be noted that, in this case, the system diverges rapidly after failure and controller must be reconfigured immediately to steer the missile using
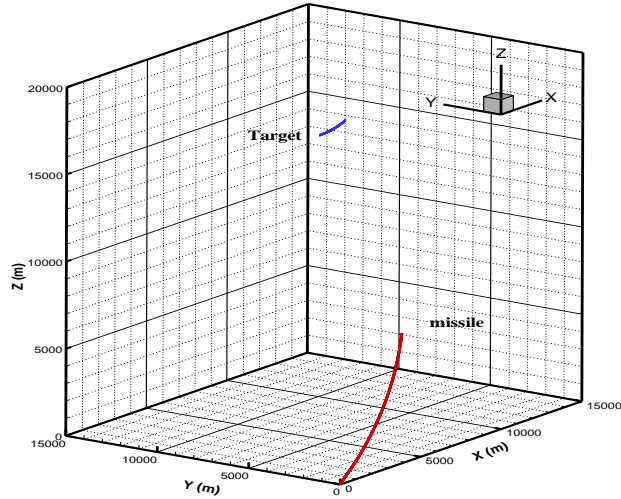
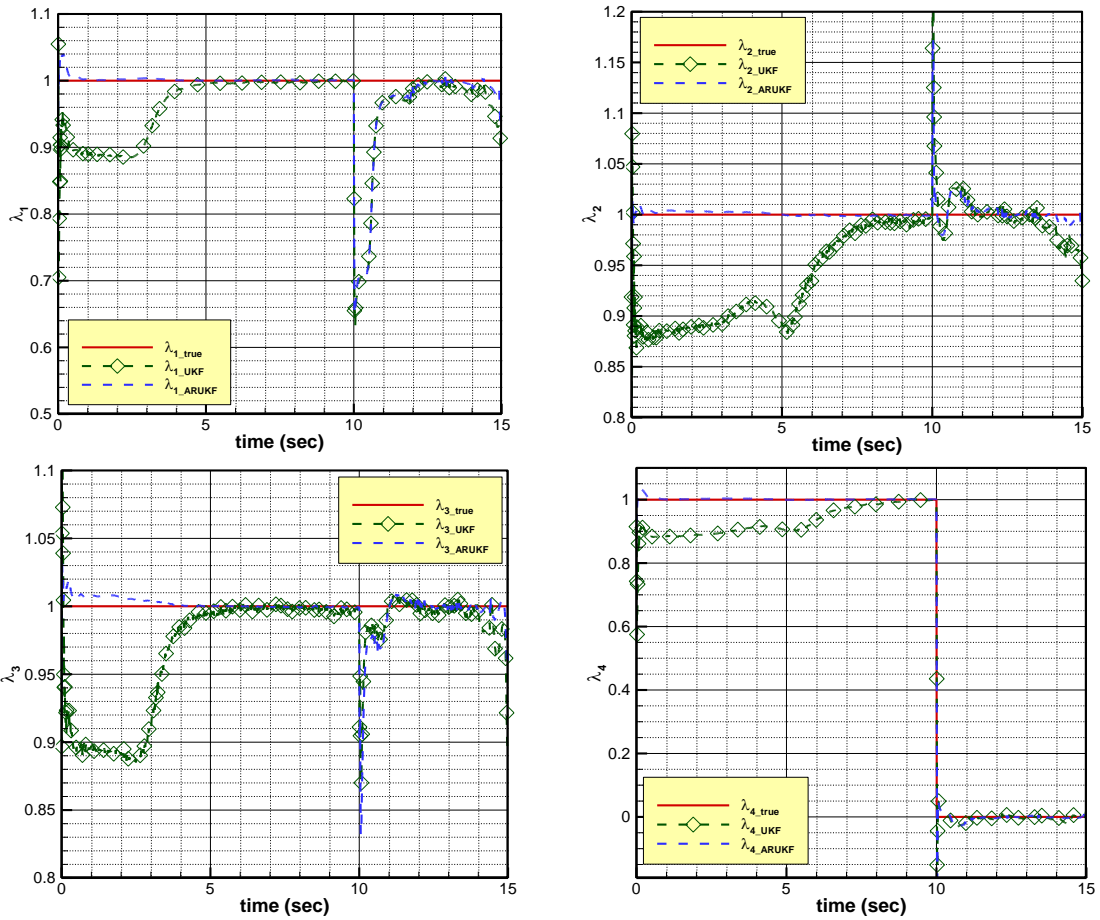Fig. 10 Missile target engagement geometry (scenario 3)

Fig. 11 Percentage of fins which have the ability to generate aerodynamic force for 1000 Monte-Carlo simulation (scenario 3)
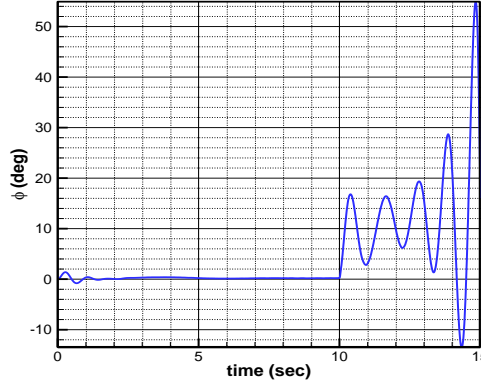
Fig. 12 Missile roll angle (scenario 3)

Table 3 The least squares error and simulation time for 1000 Monte-Carlo simulation

	Scenario 1		Scenario 2		Scenario 3	
	UKF	ARUKF	UKF	ARUKF	UKF	ARUKF
λ_1	0.4367	0.0777	1.9642	1.4699	5.7505	5.7065
λ_2	0.6522	0.1301	1.0489	0.2219	0.2999	0.2498
λ_3	0.5297	0.1865	1.6074	1.0809	0.4136	0.3344
λ_4	0.6759	0.0930	1.1609	0.2648	0.4036	0.3241
t_{run} (sec)	13.8	20.6	10.8	16.4	8.2	12.1

three remaining fins.

The least squares error of λ_i for 1000 Monte-Carlo simulation runs for all scenarios has been shown in Table 3. The results show the superiority of the Robust filter compared to conventional UKF. Moreover, although the ARUKF execution time is greater than UKF, both filters have the ability to run in real time.

6. Conclusions

In this paper, fin failure diagnosis for an agile supersonic flight vehicle using INS data is studied. An equivalent aerodynamic model is proposed which alleviates the complexity of estimating all the required aerodynamic coefficients of the controller. In this model, the aerodynamic coefficients for fins and body are modeled separately. Moreover, the health percentage of each fin is modeled as a parameter estimated by nonlinear filters. Besides, the uncertainties of the aerodynamic model and estimation errors are compensated using an adaptive robust filter. By estimating the percentage of fins which are destroyed, new aerodynamic coefficients are determined and the new model is determined after failure. The performance of the new algorithm is investigated in chase engagement scenarios. The results of Mont-Carlo simulation demonstrate that the new failure diagnosis algorithm estimates the fins health percentage accurately. Estimated values of the λ_i are sent to the controller and the controller changes the control signal accordingly. Also, the execution time of the algorithm shows that it can be implemented in real time.

References

Anguelova, M. (2004), "Nonlinear observability and identifiability: General theory and a case study of a kinetic model S. cerevisiae", Chalmers University of Technology, Göteborg, Sweden.

Basri, M.H., Lias, K., Abidin W.W.Z, Tay, K.M. and Zen, H. (2012), "Fault detection using dynamic parity space Aaproach", *Proceedings of the Power Engineering and Optimization Conference (PEDCO)*, Melaka, Malaysia.

Blanke, M. (1999), "Fault-tolerant control systems", *Adv. Control*, 171-196. https://doi.org/10.1007/978-1-4471-0853-5_6.

Chen, W.H. (2003), "Nonlinear disturbance observer-enhanced dynamic inversion control of missiles", *J. Guid. Control Dyn*., **26**(1), 161-166. https://doi.org/10.2514/2.5027.

Crassidis, J.L. and Junkins, J.L. (2004), *Optimal Estimation of Dynamic Systems*, CRC Press.

Crawford, L.S., Sharma, V. and Menon, P. (2000), "Numerical synthesis of a failure-tolerant, nonlinear adaptive autopilot", *Proceedings of the 2000 IEEE International Conference on Control Applications*, Anchorage, Alaska, U.S.A., September

Frank, P.M. (1990), "Fault diagnosis in dynamic systems using analytical and knowledge-based redundancy: A survey and some new results", *Automatica*, **26**(3), 459-474. https://doi.org/10.1016/0005-1098(90)90018-D.

Gertler, J. and Singer, D. (1990), "A new structural framework for parity equation-based failure detection and isolation", *Automatica*, **26**(2), 381-388. https://doi.org/10.1016/0005-1098(90)90133-3.

Gertler, J. (1997), "Fault detection and isolation using parity relations", *Control Eng. Practice*, **5**(5), 653-661. https://doi.org/10.1016/S0967-0661(97)00047-6.

Halder, P., Chaudhuri, S. and Mukhopadhyay, S. (2003), "Fault detection, diagnosis and control in a tactical aerospace vehicle", *Proceedings of the TENCON 2003 Conference on Convergent Technologies for the Asia Pacific Region*, Bangalore, India, October.

Hanlon, P.D. and Maybeck, P.S. (2000), "Multiple-model adaptive estimation using a residual correlation Kalman filter bank", *IEEE T. Aerosp. Electron. Syst*., **36**(2), 393-406. https://doi.org/10.1109/7.845216.

He, J., Qi, R., Jiang, B. and Zhai, R. (2017), "Fault-tolerant control with mixed aerodynamic surfaces and RCS jets for hypersonic reentry vehicles", *Chin. J. Aeronaut*., **30**(2), 780-795. https://doi.org/10.1016/j.cja.2017.01.003.

Hemsch, M. (1992), "Tactical missile aerodynamics-General topics", *Progress Astronaut. Aeronaut*., **141**.

Ishihara, S. and Yamakita, M. (2016), "Adaptive robust UKF for nonlinear systems with parameter uncertainties", *Proceedings of the IECON 2016-42nd Annual Conference of the IEEE Industrial Electronics Society*, Florence, Italy, October.

Jiang, J. and Zhao, Q. (1997), "Should we use parameter estimation or state estimation based FDI algorithms?", *IFAC Proc. Vol*., **30**(18) 459-464. https://doi.org/10.1016/S1474-6670(17)42444-X.

Johnson, D.M. (1996), "A review of fault management techniques used in safety-critical avionic systems", *Progress Aerosp. Sci*., **32**(5),415-431. https://doi.org/10.1016/0376-0421(96)82785-0.

Juan, Z. (2011), "Fault detection for nonlinear systems based on parity space approach", *Proceedings of the 30th Chinese Control Conference (CCC)*, Yantai, China, July.

Julier, S.J. and Uhlmann, J.K. (1997), "New extension of the Kalman filter to nonlinear systems", *Proceedings of the AeroSense'97: International Society for Optics and Photonics*, Orlando, Florida, U.S.A.

Kun, Q., Pang, X.P., Hao, Y. and Kai, L. (2010), "Aircraft health monitoring system using multiple-model adaptive estimation", *Proceedings of the 2010 Second WRI Global Congress on Intelligent Systems*, Wuhan, China, December.

Lee, H., Snyder, S. and Hovakimyan, N. (2014), "An adaptive unknown input observer for fault detection and isolation of aircraft actuator faults", *Proceedings of the 2014 AIAA Guidance, Navigation, and Control Conference*, National Harbor, Maryland, U.S.A., January.

Lee, H., Snyder, S., Patterson, A. and Hovakimyan, N. (2016), "Aircraft actuator fault detection and isolation using piecewise constant fault estimation scheme", *Proceedings of the 2016 AIAA Guidance,*

Navigation, and Control Conference, San Diego, California, U.S.A., January.

Lu, P., van Kampen, E., de Visser, C.C. and Chu, Q.P. (2017), "Framework for simultaneous sensor and actuator fault-tolerant flight control", *J. Guid. Control Dyn.*, **40**(8), 2133-2136. https://doi.org/10.2514/1.G002079.

Mack, S., Tao, G. and Burkholder, J.O. (2010), "Adaptive detection of aircraft actuator failures and aerodynamic damage", *Proceedings of the AIAA Guidance, Navigation and Control Conference*, Toronto, Canada, August.

Marzat, J., Piet-Lahanier, H., Damongeot, F. and Walter, E. (2009), "A new model-free method performing closed-loop fault diagnosis for an aeronautical system", *Proceedings of the 7th Workshop on Advanced Control and Diagnosis*, Zielona Gora, Poland, November.

Marzat, J., Piet-Lahanier, H., Damongeot, F. and Walter, E. (2010), "Fault diagnosis for nonlinear aircraft based on control-induced redundancy", *Proceedings of the IEEE Conference on Control and Fault-Tolerant Systems, SysTol2010*, Nice, France, October.

Marzat, J., Piet-Lahanier, H., Damongeot, F. and Walter E. (2012), "Model-based fault diagnosis for aerospace systems: a survey", *Proc. Inst. Mech. Eng. Part G J. Aerosp. Eng.*, **226**(10), 1329-1360. https://doi.org/10.1177%2F0954410011421717.

Meskin, N., Jiang, T., Sobhani, E., Khorasani, K. and Rabbath, C. (2007), "Nonlinear geometric approach to fault detection and isolation in an aircraft nonlinear longitudinal model", *Proceedings of the 2007 American Control Conference*, New York, U.S.A., July.

Patton, R.J. and Chen, J. (1994), "Review of parity space approaches to fault diagnosis for aerospace systems", *J. Guid. Control Dyn.*, **17**(2) 278-285. https://doi.org/10.2514/3.21194.

Patton, R.J. (1997), "Fault-tolerant control systems: The 1997 situation", *Proceedings of the IFAC Symposium on Fault Detection Supervision and Safety for Technical Processes*, Kingston upon Hull, U.K., August.

Rosema, C., Doyle, J., Auman, L., Underwood, M. and Blake, W.B. (2011), *Missile DATCOM User's Manual-2011 Revision*, Army Aviation and Missile Research Development ENG CTR Redstone Arsenal AL System Simulation and Development Directorate.

Shahrokhi, T.S. (2015), "Fault Detection, Isolation and Identification of Autonomous Underwater Vehicles Using Dynamic Neural Networks and Genetic Algorithms", Ph.D. Dissertation, Concordia University, Montreal, Quebec, Canada.

Simon, D. (2006), *Optimal State Estimation: Kalman, H infinity, and Nonlinear Approaches*, John Wiley & Sons.

Stevens, B.L., Lewis, F.L. and Johnson, E.N. (2015), *Aircraft Control and Simulation: Dynamics, Controls Design, and Autonomous Systems*, John Wiley & Sons.

Van Der Merwe, R., Doucet, A., De Freitas, N. and Wan, E. (2001), "The unscented particle filter", *Adv. Neural Inform. Process. Syst.*, 584-590.

Yang, X., Warren, M., Arain, B., Upcroft, B., Gonzalez, F. and Mejias, L. (2013), "A UKF-based estimation strategy for actuator fault detection of UASs", *Proceedings of the 2013 International Conference on Unmanned Aircraft Systems (ICUAS)*, Atlanta, Georgia, U.S.A., May.

Yu, C., Han, H.X. and Min, W. (2009), "Missile fault detection based on linear parameter varying fault detection filter", *Inform. Technol. J.*, **8**(3), 340-346.

Zhang, Y. and Jiang, J. (2008), "Bibliographical review on reconfigurable fault-tolerant control systems. Annual reviews in control", *Ann. Rev. Control*, **32**(2), 229-252. https://doi.org/10.1016/j.arcontrol.2008.03.008.

Zipfel, P.H. (2007), *Modeling and Simulation of Aerospace Vehicle Dynamics*, American Institute of Aeronautics and Astronautics.

GY